eng

MDPI

Article

Coupled Design and Operation Optimization for Decarbonization of Industrial Energy Systems Using an Open-Source In-House Tool

Rushit Kansara * and María Isabel Roldán Serrano

German Aerospace Center, Institute for Low-Carbon Industrial Processes, Walther-Pauer-Straße 5, 03046 Cottbus, Germany; maria.roldanserrano@dlr.de
* Correspondence: rushit.kansara@dlr.de

Abstract: The decarbonization of industrial energy systems which comprise different networks (such as steam, water, electric power, fuel sources) is crucial for mitigating climate change and achieving sustainability goals. This paper presents a comprehensive methodology integrated in an open-source in-house tool for the coupled design and operation optimization of energy systems in industrial settings. The proposed approach integrates advanced optimization techniques with modeling of energy systems including properties like mass flow and temperature to simultaneously optimize both design parameters and operational strategies. The methodology encompasses the optimized integration of various energy technologies, such as renewable energy technologies, energy storage, and power-to-heat technologies while considering changing operational conditions and variable energy demand and supply. A multi-objective optimization framework is employed to balance conflicting targets, such as minimizing greenhouse gas emissions, operational costs, and ensuring system reliability. The in-house tool application considering a case study based on a food industry process demonstrates the effectiveness of the proposed approach in significantly reducing carbon footprints as well as operational and investment costs compared to traditional low-fidelity methods incorporated in commercial tools. The optimized concept achieved through the in-house tool has shown 8.5% less emission (EMI) compared to the optimized designs of the commercial tool. It shows 36% reduction in CO_2 emissions compared to the existing facility of the case study. The optimized energy concept can be implemented in the existing facility with a payback period of 4.6 years. The outcomes of the selected use-case highlight the importance of coordinated design and operation decisions in achieving optimal performance and sustainability in industrial energy systems. It also shows an ideal workflow for making optimized design decisions to decarbonize industry with novel energy concepts. Thus, this work provides a robust foundation for future research and practical applications aimed at accelerating the transition towards low-carbon industrial processes.

Keywords: coupled optimization; modeling; decarbonization; optimal design; optimal operation strategy

Citation: Kansara, R.; Roldán Serrano, M.I. Coupled Design and Operation Optimization for Decarbonization of Industrial Energy Systems Using an Open-Source In-House Tool. *Eng* **2024**, *5*, 3033–3048. https://doi.org/10.3390/eng5040158

Academic Editors: George Z. Papageorgiou, Maria Founti and George N. Nikolaidis

Received: 17 September 2024
Revised: 10 November 2024
Accepted: 19 November 2024
Published: 22 November 2024

1. Introduction

The need for sustainable production is increasing in industries all over the world. Industries are responsible for almost 34% of the CO_2 emissions in Europe [1]. A very important challenge that must be considered for sustainable production is the reduction of the use of fossil fuels, which are currently used extensively. The associated emission of greenhouse gas needs to be mitigated due to their hazardous effects on the climate. Novel energy transition methods or concepts such as Integrated Energy System (IES) which comprises different Renewable Energy Sources (RESs), power to heat conversion components, energy storages and if needed also conventional fuel-based energy components could mitigate CO_2 emissions effectively [2]. Efficient design and operation of such energy-transition concepts is very crucial due to the economic aspects attached to it. Such optimal energy-transition

concepts have potential to support significant cost savings alongside reducing CO_2 emissions of industrial energy systems [3–5]. The design decisions, such as the capacities of the units involved and the layout of the energy system, are usually determined before the development of energy concepts. On the other hand, strategic operation decisions are required after the development of concepts, such as the operating strategy of the IES [6].

Multi-objective energy optimization to select a design and plan an operational strategy could be one of the most effective ways to solve such problems. When the design and operation of an energy system are optimized in a decoupled manner without consideration of their dependencies on each other, it could lead to suboptimal solutions [7]. Therefore, it is important to consider both design and operation, which leads to a coupled optimization problem, where the design capacity and operation of the IES have to be optimized simultaneously in order to minimize costs and CO_2 emissions [2]. Ref. [8] showed the optimal capacity and operation of storages in a multi-energy system. The optimization problem in [8] is formulated as a Mixed Integer Linear Program (MILP) and solved with Gurobi (Version 10.0) [9]. Ref. [10] optimized the design of integrated urban energy systems considering uncertainty in the renewable generation. Ref. [10] formulated an optimization problem as MILP and solved with stochastic solvers. Ref. [11] demonstrated an integrated design and operation optimization (MILP solved with Gurobi) of multi-energy systems in dairies and showed significant reduction in emissions. Apart from the above-mentioned research, there are many commercial software tools available, which perform energy system optimization and offer different functionalities [12–14]. Such traditional commercial software tools typically rely on energy-balance methods, which are mostly formulated as Linear Problems (LPs) or MILP and overlook critical thermodynamic parameters, such as mass flow rates and temperature variations across components. However, these parameters are crucial for accurately capturing exergy losses, component interactions, and the dynamic behavior of systems [15]. By integrating mass and temperature data into optimization frameworks, such as in coupled design and operation models, it becomes possible to achieve higher fidelity and more realistic system designs. These models can better account for heat-transfer characteristics, efficiency curves, and non-linearities in equipment performance, leading to more reliable and optimized energy systems [16]. Consequently, this approach not only enhances the system's overall energy efficiency but also aligns better with practical operational conditions and system constraints, which is often missed by conventional energy-balance-based tools. These problems are usually Non-Linear Problems (NLPs). As energy systems become increasingly complex, mass- and temperature-based optimization models represent a critical advancement over traditional methods, offering substantial improvements in both economic and environmental outcomes. There exist some commercial software tools that use thermodynamic properties [17–19]. These tools allow for rigorous process design and operational flexibility, which is critical in industries with complex heat and material exchanges. Energy-balance-focused tools (e.g., Top-Energy 3.2, EnergyPLAN, RETscreen) simplify the system modeling by focusing on energy inputs and outputs, making them less accurate for systems requiring detailed thermodynamic analysis. Tools like Aspen Plus V14.1 and Modelica V1.23.0 can model complex process-integration scenarios, including co-generation and heat-recovery systems, where temperature levels and mass flows are critical. In contrast, energy-balance tools focus on overall system energy efficiency, often missing opportunities for deeper integration and optimization at the thermodynamic level.

In the process of optimizing the design and operation of integrated energy systems, one efficient way to use energy-balance-based commercial tools is to simulate different configurations with commercial tools and decide on the final configuration. Simulating different configurations of energy components' connections is computationally expensive. It can be simulated with MILP frameworks of commercial tools. When the configuration is finalized, coupled design and operation optimization can be carried out with a detailed NLP optimization framework [2]. This paper explores the coupled design and operation

optimization considering non-linear thermodynamic properties' interactions, which leads to better design decisions compared to commercial tools.

2. Materials and Methods

In this paper, an in-house programmed tool is presented for coupled design and operation optimization of energy systems. Sanddorn GmbH (Herzberg, Germany), which is located in the state Brandenburg in Germany is chosen as the case study for this paper. Sanddorn GmbH is one of the partners in the European Union's Horizon Europe Project SINNOGENES. It is a medium-sized food and cosmetic industry. The energy concept is first configured and coupled design-operation optimization is performed for the case study. The problem is first formulated with the energy-balance method and optimized in Top-Energy and preliminary concepts are analyzed. Among these preliminary concepts, the most optimal and convenient concept is chosen by the stakeholder. This concept is then further implemented with detailed modeling considering thermodynamic properties such as mass flow and temperature in the in-house tool. The optimized designs are then compared with the preliminary design results of Top-Energy. The commercial software tools usually use Linear Problem (LP) and Mixed Integer Linear Problem (MILP) solvers for faster computation. Due to the large number of constraints and variables, the proposed multi-objective coupled optimization problem is very complex and requires large computational efforts. Most of the energy-balance-based energy system-optimization problems are MILP. With the inclusion of thermodynamic properties in modeling energy components and their interaction, the problem becomes a Non-Linear Problem (NLP), which is computationally quite expensive to solve. In this paper the MILP solution acquired by commercial software and the NLP solution acquired by the in-house optimization framework are compared and analyzed.

2.1. Case Study

As mentioned in Section 2, a food and cosmetic industry facility is chosen as the case study as part of teh EU Project SINNOGENES. The existing facility of the energy system of Sanddorn GmbH consists of a gas boiler for generating steam and a 55 kWp-PV plant for renewable electricity generation, which is connected to the electric grid for the feed-in electricity. The heat required for the production is covered by generating steam at 133 °C temperature and 3 bar pressure. It is further used in flash pasteurisation at 76 °C and for eliminating pathogens with thermal treatment at 90 °C. The existing components are shown in Figure 1. Current electricity and heat demand for this process are shown in Figure 2.

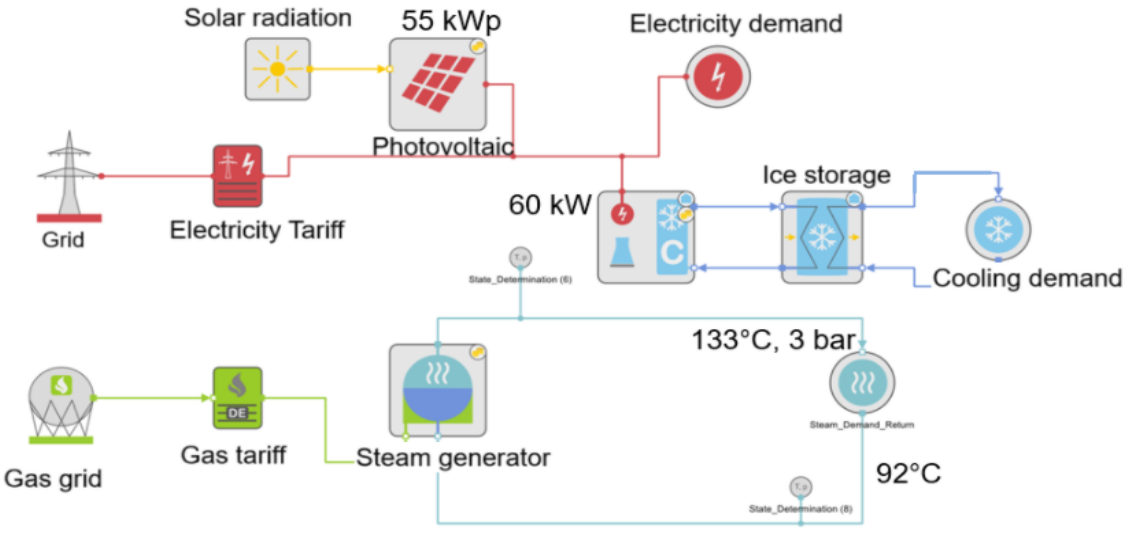

Figure 1. Existing facility of Sanddorn GmbH.

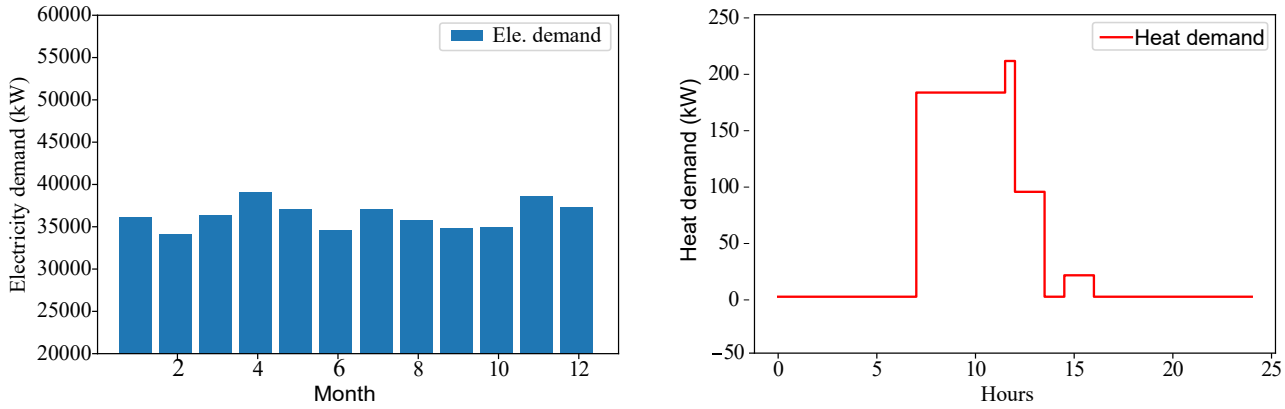

(a) Electricity demand **(b)** Heat demand

Figure 2. Electricity and heat demand of the use-case.

Table 1 shows the current operating cost and CO_2 emissions of the Sanddorn GmbH production facility for one year. The main aim of this project is to minimize these CO_2 emissions with minimum investment and operating cost.

Table 1. Operating cost (T€/a) and CO_2 emissions (t/a).

Operating Cost	CO_2 Emissions
161	217

As mentioned earlier, in the existing facility heat demand is covered by steam. The main energy-consuming unit is the flash pasteurization unit, which requires high-temperature heat for short periods of time. For this purpose, high-temperature steam has been used so far. The first step towards decarbonizing the industry was to reduce the heat demand by shifting from steam to hot water. Hot water requires higher mass flow but it reduces the high-temperature requirement. The experiments were performed at the facility and the stakeholder decided to deliver heat at 95 °C flow temperature with hot water. It reduces the heat demand up to 15%.

Table 2 shows the new operating cost and CO_2 emission when using hot water to cover heat demand instead of high temperature steam. It reduces by 4.3% and 6% the current operating cost and CO_2 emissions, respectively.

Table 2. New operating cost (T€/a) and CO_2 emissions (t/a) when using hot water to cover heat demand.

Operating Cost	CO_2 Emissions
154	204

To find the optimal design and operation of the processing plant, one superstructure was created initially with all the possible energy components available. Preliminary studies showed that the Wind Turbine (WT) does not fit in the case study due to its very high investment costs [2]. Figure 3 shows the superstructure considered for the optimization of the energy system.

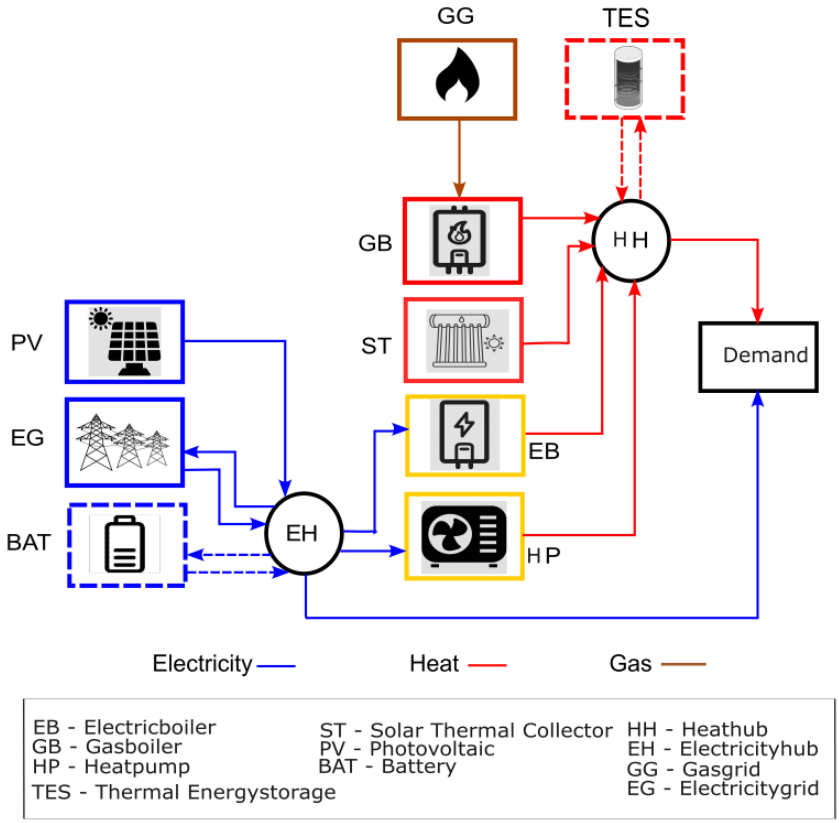

Figure 3. Superstructure for coupled optimization.

2.2. Modeling and Problem Formulation for Energy-Balance-Based Optimization

In coupled optimization, operations of the energy concept including different energy components and their capacities are optimized simultaneously. By doing this, an appropriate capacity estimation can be achieved which also includes the effects of operational strategy, which in turn support strategic decisions of the investment. Thus, optimum values of the capacities of renewable energy (RE) systems and storages in an energy concept can be determined by carrying out structural optimization [20]. First, these components are modelled in Top-Energy software. Their design and operation are optimized with MILP solver. As mentioned in Section 2, the preliminary designs for finalizing the configuration of the energy concept can be optimized with a commercial tool such as Top-Energy, and later detailed non-linear coupled optimization can be performed with an in-house tool to obtain better design capacities. The modeling of different components follows below. Modeling of the components is taken from the works of [2,20].

2.2.1. Photovoltaic

The electrical power output P_{out}^{PV} of the PV unit depends on the solar irradiance I and the efficiency of the PV unit η^{PV}. It is mainly constrained by solar irradiance I and the peak power P_{peak}^{PV}. The maximum output is restricted by the maximum peak power, which is 55 kWp, because the case study facility does not have more space available for large PV to be installed. That is why PV size is not considered as a design variable. Only power output P_{out}^{PV} of PV is taken as an operational variable in coupled optimization. It is represented by

$$P_{out}^{PV} = \eta^{PV} \cdot P_{peak}^{PV} \frac{I_g}{I_{ST}} \cdot \left(1 + TC\left(T_{cell}^{PV} - T_{ST}^{PV}\right)\right), \quad (1)$$

where η^{PV} is the collector efficiency which is chosen as constant 0.19, which is taken from the existing PV system installed in the facility; I_{ST} is the incident radiation taken for the standard test conditions (1000 W/m^2); TC represents the temperature coefficient; T_{cell}^{PV} is the

temperature of the PV_{cell}; T_{ST}^{PV} represents the temperature at the standard test conditions; and I_g represents the global inclined incidence irradiance for the location.

The peak power of the whole PV system is given by

$$P_{peak}^{PV} = P_{peak}^{m^2} \cdot A_{nom}^{PV}, \tag{2}$$

where $P_{peak}^{m^2}$ is the peak power per square meter. T_{cell}^{PV} is defined as

$$T_{cell}^{PV} = T_{amb} + \left(I_g - I_{NOCT}\right) \cdot \left(T_{NOCT}^{cell} - T_{NOCT}^{amb}\right), \tag{3}$$

where I_{NOCT} is the solar radiation. At I_{NOCT}, NCOT is defined, which stands for Nominal Cell Operating Temperature; T_{NOCT}^{cell} is the Nominal Operating Cell Temperature (318.15 k), and, T_{NOCT}^{amb} is the ambient temperature when NCOT is defined (298.15 k).

2.2.2. Electric Boiler

An EB is modelled with power-to-heat efficiency. Efficiency η^{EB} for EB is taken as constant (0.95) to have a linear relation and ease of computation [21]. The heat output of the EB generally depends on input (consumed) electric power P_{in}^{EB} to the EB, part-load behavior α^{EB}, and nominal capacity P_{nom}^{EB}, which is a design variable. It is shown as

$$P_{out}^{EB} = \eta^{EB} \cdot P_{in}^{EB}, \qquad P_{out}^{EB} = \alpha^{EB} \cdot P_{nom}^{EB}. \tag{4}$$

2.2.3. Solar Thermal Collector

There are two types of ST collectors, which are generally used for generating renewable heat, flat plate collectors and evacuated tube collectors. For this use-case, flat plate collectors with tilt angle of 40° are chosen according to the mounting space available on the facility, which is integrated in the proposed energy concept [22]. The ST model is created according to the quadratic efficiency model developed by [23], which is shown as

$$\eta^{ST} = \eta_0 - \frac{a_1 \cdot \Delta T}{I} - \frac{a_2 \cdot \Delta T^2}{I}, \tag{5}$$

where η_0 represents optical collector efficiency, a_1 and a_2 stand for loss coefficients in relation to linear and quadratic terms, ΔT shows the temperature difference between collector fluid temperature and ambient outside temperature, and I represents global solar irradiance on the flat plate collector surface for the given location. According to the European EN 19275, collector fluid temperature can be chosen as the average collector temperature of the inlet and outlet temperature of the working fluid [24].

Weather data for each hour at the location of Sanddorn GmbH were collected from European commission photovoltaic geographical information system [25].

Output thermal energy of ST is given by

$$\dot{Q}_{ST} = \eta^{ST} \cdot I \cdot A_{nom}^{ST}, \tag{6}$$

where the collector surface area A_{nom}^{ST} of the flat plate collector is the design variable.

2.2.4. Heat Pump

Thermal output power of the heat pump depends on its nominal capacity P_{nom}^{HP}, and part-load behavior λ^{HP}.

$$P_{out}^{HP} = P_{nom}^{HP} \cdot \lambda^{HP} \tag{7}$$

The coefficient of performance (COP) is calculated as

$$COP_{HP} = 0.5 \frac{T_{out}^{w}}{T_{out}^{w} - T_{source}^{c}}, \tag{8}$$

where T^{w}_{out} is the outlet temperature on the heat sink side, and T^{c}_{amb} corresponds to the heat source temperature. The efficiency is chosen as 0.5, which is usually taken as an average efficiency in different manufacturers' heat pumps [26].

Hence, the output power is defined as

$$P^{HP}_{out} = P^{HP}_{in} \cdot COP^{HP} \tag{9}$$

where P^{HP}_{in} is the input electric power.

2.2.5. Thermal Energy Storage

Energy balance for the thermal energy storage is given as

$$\frac{\mathrm{d}E^{TES}}{\mathrm{d}t} = \dot{Q}^{ch} - \dot{Q}^{dch} - \dot{Q}^{loss}, \tag{10}$$

where E is the energy stored in TES at the given time. $\dot{Q}^{ch}$ is the charging power, which is defined as

$$\dot{Q}^{ch} = \eta^{ch} \cdot P^{TES}_{ch} \tag{11}$$

where η^{ch} is the charging efficiency and P^{TES}_{ch} represents charging power.

$\dot{Q}^{dch}$ represents discharging power, which is calculated as

$$\dot{Q}^{dch} = \frac{1}{\eta^{dch}} \cdot P^{TES}_{dch}, \tag{12}$$

where η^{dch} is the discharging efficiency and P^{TES}_{dch} represents discharging power. TES is assumed as a lumped storage, where the temperature inside the storage remains constant throughout the spatial co-ordinates. This assumption is for ease of calculation. When the modeling fidelity is increased, the temperature gradient inside the storage must be considered.

2.3. Problem Formulation

The coupled design and operation optimization problem formulated for the case study has two objectives which have to be minimized: total annualized cost (TAC) and emission (EMI) [2]. TAC is the aggregation of the investment cost (C) and operational cost (OC) over one year. The production plant of the use-case is already built, so the investment cost for building the facility and land cost are excluded. EMI is the representation of the CO_2 emission. The minimization problem is formulated as

$$\min_{\mathbf{x},\mathbf{y}} [TAC(\mathbf{x},\mathbf{y}), EMI(\mathbf{x},\mathbf{y})], \tag{13}$$

with TAC and EMI as the objectives to minimize. The first minimization objective TAC includes the investment cost of each component and the operational cost of the energy system concept, which is shown as

$$TAC(\mathbf{x},\mathbf{y}) = OC(\mathbf{x},\mathbf{y}) + \sum_{i \in D} C^{i}\left(x^{i}\right), \tag{14}$$

where OC depends on the net electricity and gas bought from the grids, which is defined as

$$OC(\mathbf{x},\mathbf{y}) = \sum_{m \in M} \left(p^{el}_{buy} \cdot E^{el}_{in,m} - p^{el}_{sell} \cdot E^{el}_{out,m} \right), \tag{15}$$

and the investment cost C^{i} of each component is described as

$$C^i = \left(\frac{(\gamma+1)^\tau \cdot \gamma}{(\gamma+1)^\tau - 1} + \alpha \right) \cdot CAPEX, \tag{16}$$

which consists of capital expenditure $CAPEX$, maintenance cost factor for operation α, interest rate γ and time horizon of the investment τ for financing the cost [2]. $CAPEX$ calculation depends on reference capacity x^i of each component and it is shown as

$$CAPEX = CAPEX^0 \cdot \left(\frac{x^i}{x^0} \right)^\beta, \tag{17}$$

where β represents the scaling exponent with respect to the nominal capacity of each energy component [21]. The second minimization objective EMI is presented as

$$EMI(\mathbf{x}, \mathbf{y}) = \sum_{m \in M} \left(g^{el} \cdot \left(E^{el}_{in,m} - E^{el}_{out,m} \right) \right), \tag{18}$$

where M represents reference days and $D = \{PV, ST, EB, HP, TES\}$.

$\mathbf{x} = \left[A^{PV}, P^{WT}_{nom}, Q^{EB}_{nom}, Q^{HP}_{nom} \right]$ are the design variables and $\mathbf{y} = \left[E^{el}_{in,m}, E^{el}_{out,m} \right]$ are the operational variables considered for the above-mentioned objective function. EMI is calculated based on how much net electricity and gas are bought from the grid. Each consumed unit of electricity $E^{el}_{in,m} - E^{el}_{out,m}$ has related corresponding CO_2 factor g^{el} for the calculation of EMI.

The heat-demand constraint is defined as

$$Q^{dem} - \left(Q^{ST} + Q^{EB} + Q^{HP} + Q^{dch} - Q^{ch} \right) \leq 0, \tag{19}$$

which shows that net heat generated from ST, EB, TES, and HP should cover the heat demand of the production process in each time step. The lower and upper bound of the capacity constraint are as follows

$$x^i_{min} \cdot z^i \leq x^i \leq x^i_{max} \cdot z^i \qquad \forall i \in \mathbf{x} \quad and \quad z^i \in \{0, 1\}, \tag{20}$$

where x^i_{min} and x^i_{max} are the lower and upper bounds of the design capacity of each energy component. z shows the the existence of the component in the energy concept as a binary variable.

Capacity limits of the energy components are shown in Table 3. These are taken as the lower and upper bounds of design variables. The PV system is already built on the existing facility and the stakeholder has decided not to extend the capacity of PV, so its lower and upper bounds are kept the same, 55 kWp. The peak heat demand as shown in Figure 2 is 209 kW. The heat-generating components' capacity bounds are chosen accordingly to fulfil this peak demand. The HP upper bound is chosen higher compared to EB, in order to charge TES with HP when electricity prices are lower. The upper limit of ST size is decided based on the space available for the mounting on the facility.

Table 3. Design capacity limits.

Component Parameter	Lower Bound	Upper Bound
PV-capacity (kWp)	55	55
ST-surface (m^2)	0	135
Electric Boiler (kW_{th})	0	250
Heat Pump (kW_{th})	0	750
TES (kW_{th})	0	1000
Battery (kWh)	0	1000

2.4. Energy-Balance-Based Optimization—MILP

As discussed earlier, the initial concepts were optimized with the commercial software Top-Energy, which is based on MILP optimization solvers. As the optimization method solves energy balance, the output temperature and mass flow cannot be varied easily at the same time. Due to this, the output temperature of each component is kept fixed at 95 °C, which is the process demand temperature. With commercial software tools, usually the design and operation variables are optimized in a decoupled manner, which might give suboptimal solutions. Due to its linear formulation, the results can be achieved faster, which is an advantage for any stakeholder with respect to making decisions.

Figure 4 shows the new optimized energy concept of the case study. This configuration is the result of the MILP (solver—GUROBI) energy-based design optimization [9]. Here, operation optimization has been partially considered with reference days. Once the capacity of the components is optimized, they are kept fixed during full operation optimization. The optimized capacity of the components can be seen in Figure 4. There are two TESs in the final concept. TES-1 will be charged by ST during hot summer days. It can also become discharged and cover the heat demand during summer days. In winters, the output temperature of ST might not reach 95 °C, which is needed to cover the heat demand. In this case, TES-1 will be used to store low-temperature ST output and use it as a heat source for the HP to increase its COP. TES-2 is majorly used to become charged by HP when the electricity prices are very low or the PV electric output is high on summer days.

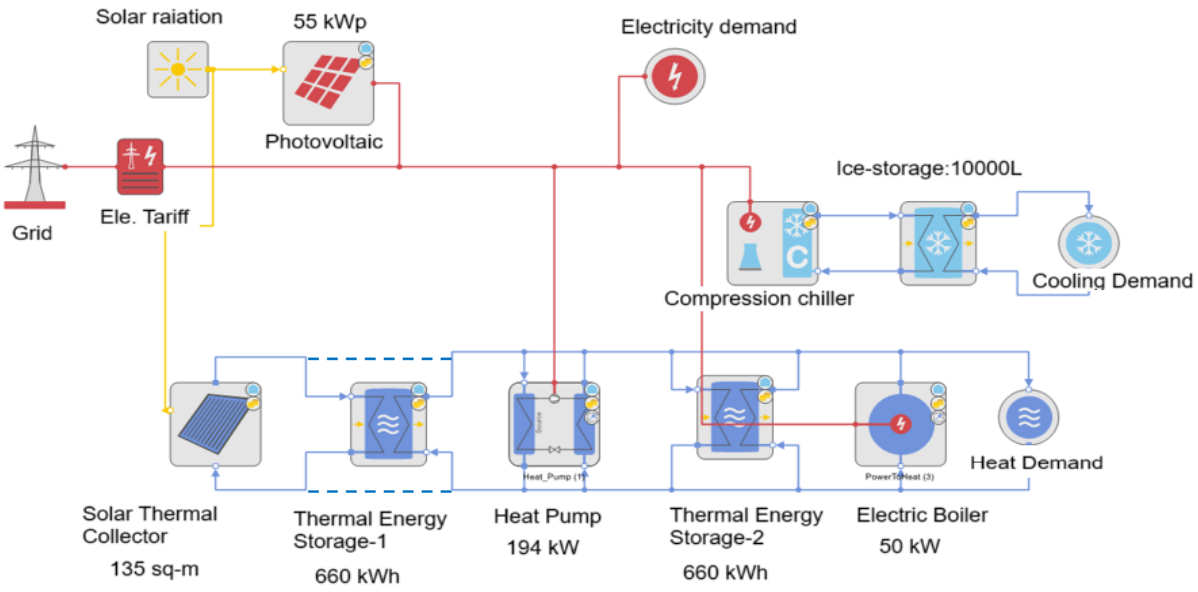

Figure 4. New energy concept of Sanddorn GmbH.

These design capacities are based on energy-balance-based optimization and linearized problem formulation. To find and validate the optimal design capacities, non-linear coupled optimization is important. In the next section, the in-house coupled optimization tool is discussed.

2.5. Coupled Design and Operation-Optimization Tool (CoDeOpT)

The Coupled Design and Operation-Optimization Tool (CoDeOpT) for energy systems integrates the process of designing energy system components with their operational strategies to maximize overall efficiency and performance. This tool simultaneously considers the selection, sizing, and configuration of system elements (such as renewable energy sources, energy-conversion and -storage systems, as well as conventional generators) and their day-to-day operational management. By optimizing both the design and operation in a unified framework, the tool ensures that the energy system can meet demand reliably,

minimize costs, and reduce environmental impact, thus providing a holistic approach to energy system planning and management in the retrofit of energy-supply systems required for an effective energy transition. This tool integrates the modeling of components with thermodynamic properties such as mass flow and temperature, which allows the component modeling to be non-linear and potentially accurate. With this approach, the output temperature and mass flow of each component can be variable in each time step. It represents more accurate mixing of energy flows in the energy system.

Three components where thermal properties are important to be considered are HP, TES, and ST. The new detailed modeling of these components for the in-house tool is explained in the next subsections.

2.5.1. Solar Thermal Collector (ST)

Incidence-correction factor for ST

$$K_{\mathrm{ST}}(t) = \cos(\theta_{\mathrm{ST}}(t)) - \Big(\alpha_{\mathrm{ST},1}\cdot\theta_{\mathrm{ST}}(t) + \alpha_{\mathrm{ST},1}\cdot\theta^2_{\mathrm{ST}}(t)\Big); \tag{21}$$

Modified incedence-correction factor for ST

$$K_{\mathrm{ST}}(t) = 1 - \frac{(1-\alpha_{\mathrm{ST}})}{0.55}\cdot\left(\frac{1}{\cos(\theta_{\mathrm{ST}}(t))} - 1\right); \tag{22}$$

Temperature difference short form

$$\Delta T_{\mathrm{ST,amb}}(t) = \frac{T_{\mathrm{ST,out}}(t) + T_{\mathrm{ST,in}}(t)}{2} - T_{\mathrm{amb}}(t); \tag{23}$$

Thermal output of ST

$$\begin{aligned}\dot{m}_{\mathrm{ST}}(t)\cdot c_{\mathrm{p,water}}\cdot(T_{\mathrm{ST,out}}(t) - T_{\mathrm{ST,in}}(t)) = {} & (1 - f_{\mathrm{ST,cur}}(t))\cdot A_{\mathrm{ST}}\cdot \\ & [K_{\mathrm{ST}}(t)\cdot I(t)\cdot\eta_{\mathrm{ST,opt}} - \\ & \beta_{\mathrm{ST},0}\cdot(\beta_{\mathrm{ST},1}\cdot\Delta T_{\mathrm{ST,amb}}(t) \\ & +\beta_{\mathrm{ST},2}\cdot\Delta T^2_{\mathrm{ST,amb}}(t) \\ & +\beta_{\mathrm{ST},3}\cdot\Delta T^3_{\mathrm{ST,amb}}(t) \\ & +\beta_{\mathrm{ST},4}\cdot\Delta T^4_{\mathrm{ST,amb}}(t)\Big)].\end{aligned}$$

2.5.2. Heat Pump (HP)

The coefficient of Performance of HP is given by

$$COP_{\mathrm{HP,hot}}(t) = \eta_{\mathrm{HP}}\cdot\frac{T_{\mathrm{HP,hot,out}}(t)}{T_{\mathrm{HP,hot,out}}(t) - T_{\mathrm{HP,cold,in}}(t)}. \tag{24}$$

The thermal output of HP is calculated with mass flow and temperature as follows

$$\dot{m}_{\mathrm{HP,hot}}(t)\cdot c_{\mathrm{p,water}}\cdot(T_{\mathrm{HP,hot,out}}(t) - T_{\mathrm{HP,hot,in}}(t)) = COP_{\mathrm{HP,hot}}(t)\cdot P_{\mathrm{HP}}(t). \tag{25}$$

The maximum thermal output power of HP is constrained as follows

$$\dot{m}_{\mathrm{HP,hot}}(t)\cdot c_{\mathrm{p,water}}\cdot(T_{\mathrm{HP,hot,out}}(t) - T_{\mathrm{HP,hot,in}}(t)) \le \dot{Q}_{\mathrm{HP,nom}}\cdot f_{\mathrm{HP,max}}. \tag{26}$$

The thermal input of HP from the heat source is given as

$$\dot{m}_{\mathrm{HP,cold}}(t)\cdot c_{\mathrm{p,water}}\cdot(T_{\mathrm{HP,cold,in}}(t) - T_{\mathrm{HP,cold,out}}(t)) = (COP_{\mathrm{HP,hot}}(t) - 1)\cdot P_{\mathrm{HP}}(t). \tag{27}$$

2.5.3. Thermal Energy Storage (TES)

The TES energy-balance equation is shown as

$$m_{\mathrm{TES}} \cdot c_{\mathrm{p,TES}} \cdot \frac{\mathrm{d}T_{\mathrm{TES}}(t)}{\mathrm{d}t} = \dot{m}_{\mathrm{TES,ch}}(t) \cdot c_{\mathrm{p,water}} \cdot (T_{\mathrm{TES,ch,in}}(t) - T_{\mathrm{TES,ch,out}}(t)) - \dot{m}_{\mathrm{TES,dis}}(t) \cdot c_{\mathrm{p,water}} \cdot (T_{\mathrm{TES,dis,out}}(t) - T_{\mathrm{TES,dis,in}}(t)). \quad (28)$$

Charging outlet temperature using an effectiveness model is represented as

$$T_{\mathrm{TES,ch,out}}(t) = T_{\mathrm{TES,ch,in}}(t) - \varepsilon_{\mathrm{TES,ch}} \cdot (T_{\mathrm{TES,ch,in}}(t) - T_{\mathrm{TES}}(t)), \quad (29)$$

where effectiveness ε is assumed to be 0.9 [27].

In the same way, discharging outlet temperature using an effectiveness model can be written as

$$T_{\mathrm{TES,dis,out}}(t) = T_{\mathrm{TES,dis,in}}(t) - \varepsilon_{\mathrm{TES,dis}} \cdot (T_{\mathrm{TES,dis,in}}(t) - T_{\mathrm{TES}}(t)). \quad (30)$$

All the symbols and parameters can be found in the "Nomenclature" list at the end of the paper.

2.6. Information Flow and Structure of the Tool (NLP)

Figure 5 shows the structure and information flow of the tool. It is divided into five major blocks, which are inputs, initialization, optimization framework, component models and post-processing (KPI-evaluation and results). This tool takes different input parameters, such as weather conditions according to location, electricity price, variable heat demand, capacity bounds, fluid properties, etc. The optimization framework handles the design and operation optimization in a coupled manner. Design optimization is solved with the genetic algorithm Non-Sorting Genetic Algorithm (NSGA-II) [28] and the operation optimization is solved inside the design optimization with the stochastic NLP solver Interior Point OPTimizer (IPOPT). The design optimization is programmed and solved in the PYMOO framework of Python (Version 3.9) and the operation optimization in the PYOMO framework of Python [28,29]. Middleware is also implemented in the tool to facilitate data exchange between the optimizer and the operator.

Some features of CoDeOpT are presented below.

- This tool integrates both the design and operational optimization processes for energy systems. It aims to minimize overall cost and emission by considering multiple energy sources, storage options, and operational strategies.
- Input data handling—the tool takes weather data inputs to assess the availability of renewable energy sources such as solar and wind. It processes electricity price data to determine optimal operation times based on market conditions. Design bounds for system components are defined to ensure feasible and practical design solutions.
- Modules—different component-modeling modules with several module connections have been created. The implemented modeling modules are as follows: Photovoltaic (PV), Solar Thermal Collector (ST), Heat Pump (HP), Thermal Energy Storage (TES), Electric Boiler (EB) and Grid. Further developments in these modules can be easily integrated.
- Optimization core—the tool uses advanced optimization algorithms to determine the optimal configuration of energy system components. It simultaneously optimizes the operation of the system to meet energy demand while minimizing costs and emissions. Both design variables (e.g., capacity, sizing) and operational variables (e.g., dispatch) are considered.
- Key Outputs:
  - Optimized design capacities: These provide the best possible sizes and configurations for various energy system components.

- Optimal operation strategy: This suggests the most efficient operational schedules and strategies to meet energy demand.
- Evaluation of Key Performance Indicators (KPIs): This calculates metrics such as savings, and emission reductions to evaluate the system's performance.

- Flexibility and adaptability—the tool is designed to handle a wide range of energy systems, including hybrid systems that combine renewable and conventional energy sources. It can be adapted to various industrial processes and scales, from small-scale installations to large industrial plants.
- It provides a user-friendly script for input data entry and parameter adjustments. It generates detailed output data files and visualizations to help users understand the optimization results and make informed decisions.
- Overall, this coupled design and operation-optimization tool provides a comprehensive solution for enhancing the performance and sustainability of energy systems, ensuring that they meet demand reliably, cost-effectively, and with minimal environmental impact.

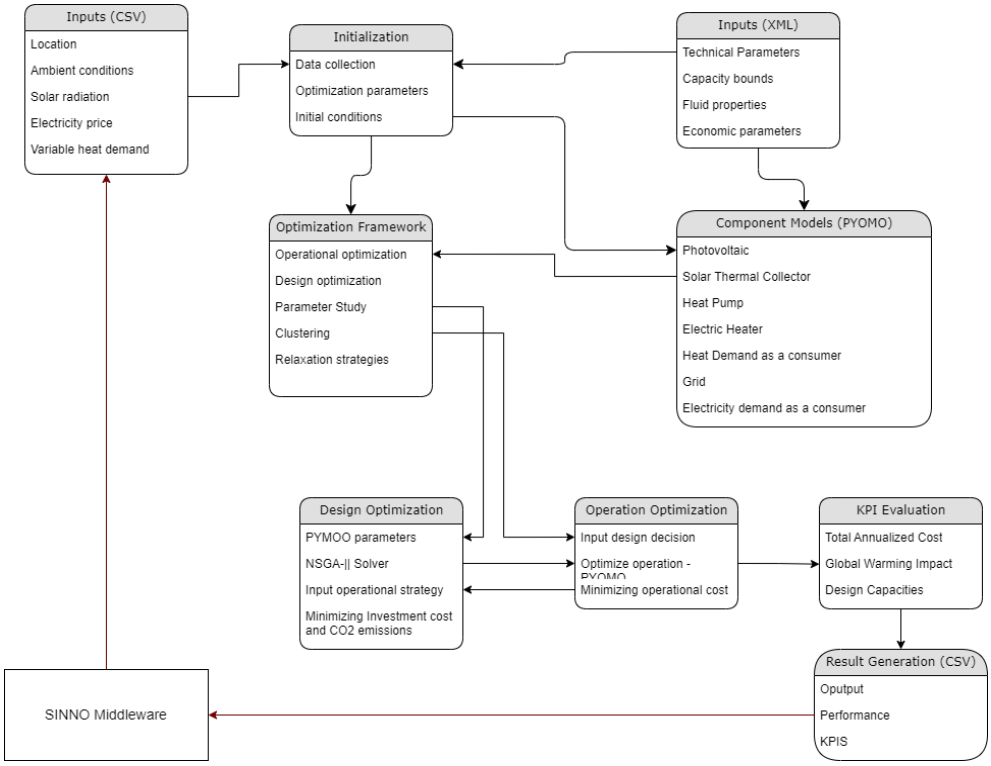

Figure 5. Tool information flow.

3. Results and Discussion

As discussed in Section 2, the commercial tool is used initially to determine the best suitable configuration from the available technology. Once the configuration is decided, MILP optimization is performed with a commercial tool to obtain the optimal designs considering some aspects of plant operation. These optimized designs might be the suboptimal solution and it has to be compared and validated with the detailed couple optimization. As explained in Section 2.5, the tool CoDeOpT allows the non-linear modeling and consideration of thermodynamic properties in solving coupled design and operation optimization. It considers the operational variables and their effects while optimizing designs in a coupled manner, which leads to better design capacities. In Figure 6, optimized design capacities that resulted from Top-Energy and CoDeOpT are compared. As can be seen in Figure 6, there is some difference between optimized capacities from MILP decoupled and NLP coupled optimization. This difference results in significant differences in optimization

objectives. NLP coupled optimization considers all non-linearities occurring in the system with the interaction of thermodynamic properties of different streams, which in turn gives better estimation of the design capacities. These design capacities lead to lesser TAC and EMI compared to the designs optimized by commercial MILP tools.

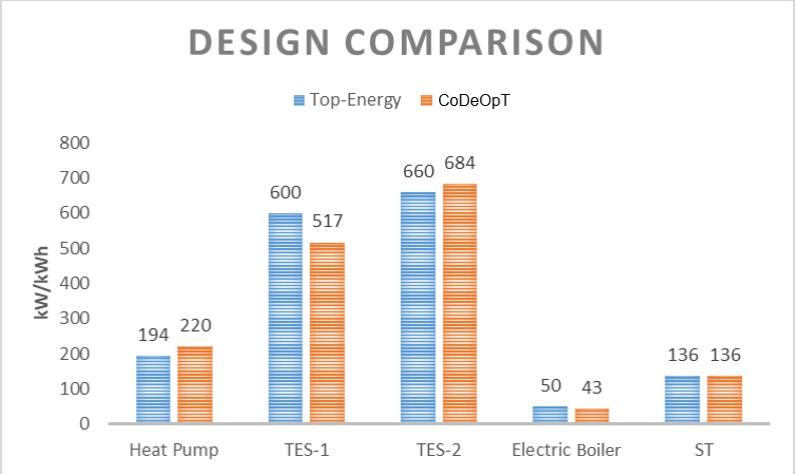

Figure 6. Design capacity comparison between MILP decoupled (Top-Energy) vs. NLP coupled (CoDeOpT) optimization.

Table 4 shows the TAC and EMI as a result of MILP decoupled optimization and NLP coupled optimization it. It also shows the reduction in TAC and EMI for optimized designs obtained from MILP and NLP optimization compared to the existing facility. It can be seen that NLP coupled optimization delivers almost 8.5% less TAC and EMI compared to MILP decoupled optimization with optimal designs. The optimized concept through NLP coupled optimization shows 36% less CO_2 emission compared to the existing facility, which can be reduced only 24% when MILP decoupled optimization is used. The payback period of the investment for the new optimized energy concept is 6.2 years when it is optimized with the MILP decoupled optimization. It is calculated to be 4.6 years, when optimized with NLP coupled optimization. Clearly, NLP coupled optimization delivers better results than MILP decoupled optimization. The drawback of NLP coupled optimization is the computational effort. NLP coupled optimization takes approximately 13 h to solve on 11th Gen Intel(R) Core(TM) i7-1185G7 with 16 GB RAM, and MILP decoupled optimization requires approximately 17 minutes on the same computer. It is a trade-off between accuracy and computational effort. NLP coupled optimization produces better results in terms of minimizing objectives, but it requires more computational effort. This can be further improved with better parallelization methods and using relaxation strategies. The results clearly show that inclusion of thermodynamic properties and non-linearity into coupled optimization delivers optimal design capacities compared to energy-balance-based linear optimization, which in turn reduces cost and emission. The MILP optimization approach overestimates the capacities due to a lack of information concerning the thermal behavior of the system. This in turn causes an overestimation of the operating cost and leads to a longer payback period. The ideal approach to make optimized design decisions according to the results of this paper is to start with the MILP commercial tool and simulate different configurations to find the best suitable configuration of the energy concept. Once the configuration is decided, one can run coupled design and operation optimization with the NLP tool. This methodology or the workflow can be the best trade-off between accuracy and computational time. This approach can be applied to different industrial use-cases as well. In an ongoing analysis of different industries, a new energy concept of a large paper-manufacturing plant optimized with NLP coupled optimization approach showed 62% reduction in CO_2 emissions compared to its existing emissions.

Table 4. TAC (T€/a) and EMI (t/a) comparison between MILP decoupled and NLP coupled optimization and the existing concept solution.

Status Quo/Tool and Solver	TAC (T€/a)	EMI (t/a)	Reduction EMI	Computational Time (h)
Existing facility	-	217	0%	-
Optimized concept with Top-Energy (MILP)	179	164	24%	0.3
Optimized concept with CoDeOpT (NLP)	152	139	36%	13

The ideal workflow to select the suitable configuration and optimize the design capacities is shown in Figure 7. It shows the steps to follow for selecting the best suitable configuration with a commercial MILP tool and running coupled NLP optimization to optimize the design capacities. This workflow takes advantage of both commercial MILP tools and the in-house NLP tool to find the best trade-off between computational time and accuracy.

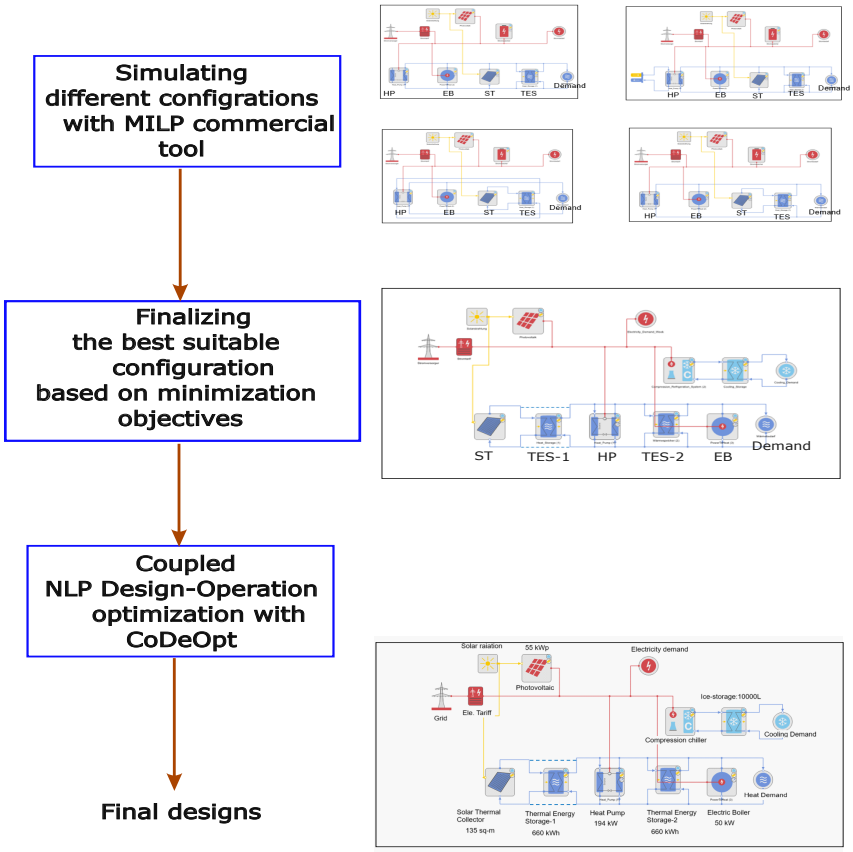

Figure 7. Workflow for selecting suitable configuration and making design decisions.

4. Conclusions

This paper presents a comparison between the commercial tool and in-house tool approach to solve a multi-objective design and operation optimization of a food industry. Component modeling for solving energy-balance-based optimization is described. This energy-balance-based approach is solved with the MILP solver to achieve computationally faster design concepts. But it might have delivered suboptimal solutions due to the linearized problem and decoupled optimization. The in-house tool CoDeOpT is introduced to solved coupled design and operation optimization for energy systems considering non-linearities in thermodynamic properties with NLP solvers. The differences in the optimized designs with respect to their effects on the minimization objectives are also presented. With NLP coupled optimization, 8.5% lower objectives compared to MILP decoupled

optimization can be achieved and it shows 36% reduction in CO_2 emission compared to the existing reference scenario (existing facility). The payback period for the proposed optimization concept is 4.6 years. An ideal workflow is shown to follow for selecting suitable configuration for the use-case and optimizing design capacities of selected energy components. The next steps in this research could be optimizing operational strategy with high accuracy. The selected design capacities were optimized considering the operational effects. The operating strategy can be further improved with high-fidelity models of thermal producers such as HP, TES, and ST, which have high interaction of thermal streams. The operating strategy can be validated with the experimental results after implementing the proposed energy components in the facility.

Author Contributions: R.K.: conceptualization, methodology, validation, investigation, data curation, writing—original draft, visualization; M.I.R.S.: project administration, supervision, reviewing. All authors have read and agreed to the published version of the manuscript.

Funding: This research was funded by the European Union's Horizon Europe project SINNOGENES (Storage innovations for green energy systems), under Grant Agreement No. 101096992.

Institutional Review Board Statement: Not applicable.

Informed Consent Statement: Not applicable.

Data Availability Statement: Restrictions apply to the availability of these data. Data were obtained from Sanddorn GmbH and are available from the authors with the permission of Sanddorn GmbH.

Acknowledgments: We would like to thank Sanddorn GmbH, Herzberg, Germany, for providing data and their continuous support.

Conflicts of Interest: The authors declare no conflicts of interest.

Nomenclature

The following abbreviations are used in this manuscript:

Letter symbols

DLR	German Aerospace Center
ST	Solar thermal collector
HP	Heat pump
TP	Thermal Producer
TES	Thermal energy storage
HTF	Heat transfer fluid
EG	Electricity grid
EB	Electric Boiler
GG	Gas grid
PV	Photovoltaic
ch	Charge
dis	Discharge
amb	Ambient
COP	Coefficient of performance
NLP	Non-linear programming
MILP	Mixed Integer Linear Programming
IPOPT	Interior Point OPTimizer
NSGA	Non-Sorting Genetic Algorithm
IR	Interest rate
LT	Life time

References

1. Voll, P.; Klaffke, C.; Hennen, M.; Bardow, A. Automated superstructure-based synthesis and optimization of distributed energy supply systems. *Energy* **2013**, *50*, 374–388. [CrossRef]
2. Kansara, R.; Lockan, M.; Roldán Serrano, M.I. Combined Physicsand Data-Driven Modeling for theDesign and Operation Optimization ofan Energy Concept Including a StorageSystem. *Energies* **2023**, *17*, 350. [CrossRef]

3. Aguilar, O.; Perry, S.J.; Kim, J.-K.; Smith, R. Design and optimization of flexible utility systems subject to variable conditions. *Chem. Eng. Res. Des.* **2007**, *85*, 1149–1168. [CrossRef]
4. Velasco-Garcia, P.; Varbanov, P.S.; Arellano-Garcia, H.; Wozny, G. Utility systems operation: Optimisation based decision making. *Appl. Therm. Eng.* **2011**, *31*, 3196–3205. [CrossRef]
5. Tina, G.M.; Passarello, G. Short-term scheduling of industrial co-generation systems for annual revenue maximisation. *Energy* **2012**, *42*, 46–56. [CrossRef]
6. Barton, P.; Li, X. *Optimal Design and Operation of Energy Systems under Uncertainty*; International Symposium on Dynamics and Control of Process Systems: Mumbai, India, 2013.
7. Patwal, R.S.; Narang, N. Multi-objective generation scheduling of integrated energy system using fuzzy based surrogate worth trade-off approach. *Renew. Energy* **2020**, *156*, 864–882. [CrossRef]
8. Bruno, S.; Dicorato, M.; Scala, M.L.; Sbrizzai, R.; Lombardi, P.A.; Arendarski, B. Optimal Sizing and Operation of Electric andThermal Storage in a Net Zero Multi Energy S. *Energies* **2019**, *12*, 3389. [CrossRef]
9. Non-Convex Quadratic Optimization. Available online: https://www.gurobi.com/events/non-convex-quadratic-optimization/ (accessed on 27 February 2023).
10. Chen, Z.; Avraamidou, S.; Li, Z.; Ni, W.; Pistikopoulos, E.N. Optimal design of integrated urban energy systems under uncertaintyand sustainability requirements. *Comput. Chem. Eng.* **2021**, *155*, 107502. [CrossRef]
11. Foslie, S.S.; Knudsen, B.R.; Korpås, M. Integrated design and operational optimization of energy systems in dairies. *Energy* **2023**, *281*, 128242. [CrossRef]
12. Gesellschaft zur Förderung Angewandter Informatik (GFaI) e.V., Top-Energy Documentation. 2024. Available online: https://topenergy.gfai.de/documentation/3-0/ (accessed on 1 November 2024).
13. Natural Resources Canada. 2021. Available online: https://natural-resources.canada.ca/maps-tools-and-publications/tools/modelling-tools/retscreen/7465 (accessed on 1 November 2024).
14. Lund, H.; Thellufsen, J.Z.; Østergaard, P.A.; Sorknaes, P.; Skoy, I.R.; Mathiesen, B.V. EnergyPLAN—Advanced analysis of smart energy systems. *Smart Energy* **2021**, *1*, 100007. [CrossRef]
15. Tsatsaronis, G. Thermo economic analysis and optimization of energy systems. *Prog. Energy Combust. Sci.* **1993**, *19*, 227–257. [CrossRef]
16. Papoulias, S.A.; Grossmann, I.E. A structural optimization approach in process synthesis-II. *Comput. Chem. Eng.* **1983**, *7*, 707–721. [CrossRef]
17. Aspen Technology. Aspen Plus®: Process Simulation Software. 2023. Available online: https://www.aspentech.com/ (accessed on 1 November 2024).
18. Process Systems Enterprise. gPROMS®: Advanced Process Modeling. 2022. Available online: https://www.siemens.com/de/de/produkte/automatisierung/industrie-software/gproms-digital-process-design-and-operations.html (accessed on 10 May 2024).
19. Dassault Systèmes. Dymola®: Multi-Domain Modeling and Simulation. Retrieved from Dassault Systèmes. 2023. Available online: https://www.3ds.com/products/catia/dymola (accessed on 8 May 2024).
20. Roldán, M.I.; Kansara, R. Optimal energy concept for decarbonisation of sea-buckthorn processing plants. *Renew. Energy Power Qual. J. (REPQJ)* **2024**, *22*, 33–38. [CrossRef] [PubMed]
21. Sass, S.; Faulwasser, T.; Hollermann, D.E.; Kappatou, C.D.; Sauer, D.; Schutz, T.; Shu, D.Y.; Bardow, A.; Groll, L.; Hagenmeyer, V.; et al. Model compendium, data, and optimization benchmarks for sector-coupled energy systems. *Comput. Chem. Eng.* **2020**, *135*, 106760. [CrossRef]
22. Grahovac, M.; Liedl, P.; Frisch, J.; Tzscheutschler, P. *Simplified Solar Collector Model: Hourly Simulation of Solar Boundary Condition for Multi-Energy Optimization*; International Congress on Heating, Refrigerating and Air-Conditioning: Belgrade, Serbia, 2011.
23. Duffie, J.; Beckman, W.A. *Solar Engineering of Thermal Processes*; John Wiley and Sons Inc.: Hoboken, NJ, USA, 1991.
24. *DIN EN 12975*; Thermische Solaranlagen und Ihre Bauteile—Kollektoren—Teil 2: Prüfverfahren. Available online: https://www.baunormenlexikon.de/norm/din-en-12975/59b89111-9fc8-4f53-9a37-9cc254ccab7c (accessed on 14 May 2024).
25. EU-Science-Hub. Photovoltaic Geographical Information System. 2020. Available online: https://joint-research-centre.ec.europa.eu/pvgis-online-tool/pvgis-tools/hourly-radiation_en (accessed on 20 January 2023).
26. Schlosser, F.; Jesper, M.; Vogelsang, J.; Walmsley, T.G.; Arpagaus, C.; Hesselbach, J. Large-scale heat pumps: Applications, performance, economic feasibility and industrial integration. *Renew. Sustain. Energy Rev.* **2020**, *133*, 110219. [CrossRef]
27. Walden, J.V.M.; Bähr, M.; Glade, A.; Gollasch, J.; Tran, A.P.; Lorenz, T. Nonlinear operational optimization of an industrial power-to-heat systemwith a high temperature heat pump, a thermal energy storage and windenergy. *Appl. Energy* **2023**, *344*, 121247. [CrossRef]
28. Slowik, A.; Kwasnicka, H. Evolutionary algorithms and their applications to engineering problems. *Neural Comput. Appl.* **2020**, *2*, 12363–12379. [CrossRef]
29. Langiu, M.; Shu, D.Y.; Baader, F.J.; Hering, D.; Bau, U.; Xhonneux, A.; Müller, D.; Bardow, A.; Mitsos, A.; Dahmen, M. Comando: A next-generation open-source framework for energy systems optimization. *Comput. Chem. Eng.* **2021**, *152*, 107366. [CrossRef]